Solar-Terrestrial Physics. 2022. Vol. 8. Iss. 1. P. 3–18. DOI: 10.12737/stp-81202201. © 2022
O.S. Mikhailova, D.Yu. Klimushkin, P.N. Mager. Published by INFRA-M Academic Publishing House

UDC 533.951.2
DOI: 10.12737/stp-81202201

Received July 23, 2021
Accepted November 09, 2021

THE CURRENT STATE OF THE THEORY OF Pc1 RANGE ULF PULSATIONS IN MAGNETOSPHERIC PLASMA WITH HEAVY IONS: A REVIEW

O.S. Mikhailova
Institute of Solar-Terrestrial Physics SB RAS, Irkutsk, Russia, o_mikhailova@iszf.irk.ru

D.Yu. Klimushkin
Institute of Solar-Terrestrial Physics SB RAS, Irkutsk, Russia, klimush@iszf.irk.ru

P.N. Mager
Institute of Solar-Terrestrial Physics SB RAS, Irkutsk, Russia, p.mager@iszf.irk.ru

Abstract. The review considers the current state of the theory of short-period ULF waves in plasma with admixture of heavy ions (ions whose mass significantly exceeds the mass of protons). The presence of heavy ions influences the spectrum and propagation characteristics of waves in Pc1 range. We examine elements of the theory of quasi-parallel and quasi-perpendicular short-period ULF waves. It is usually suggested that quasi-parallel ion-cyclotron waves have a left circular polarization. Quasi-perpendicular ion-ion hybrid waves have linear polarization and can be poloidal and toroidal. We discuss the theory of an equatorial resonator for Pc1 waves and determine its size from the density of heavy ions. In the radial direction, the waves can be locked in the vicinity of the plasmapause or in the region of a local minimum in the density of heavy ions. The equatorial resonator for arbitrary values of the wave vector components is considered. We note that ion-ion hybrid waves, in contrast to Alfvén waves, have a large parallel component of the magnetic field.

Keywords: Pc1 geomagnetic pulsations, ULF waves, ion-ion hybrid waves, multicomponent plasma, heavy ions.

INTRODUCTION

Ultra-low frequency (ULF) waves are continuously observed in Earth's magnetosphere. They are usually classified as short-period (Pc1-2 and Pi1) and long-period (Pc3-5 and Pi2) waves. The most high-frequency of them are geomagnetic pulsations Pc1 (0.2–5 Hz). They play an important role in various magnetospheric processes, in particular in the magnetosphere-ionosphere coupling [Demekhov, 2012; Fedorov et al., 2016; Mishin et al., 2020], in the enrichment of the magnetosphere by heavy ions during substorms [Horne and Thorne, 1997], in the enhancement of proton precipitation [Lessard et al., 2011; Mishin et al., 2018], and in the acceleration of charged particles [Engebretson et al., 2007; Usanova et al., 2014]. Of the Pc1 pulsations, oscillations of a special type stand out whose sonogram resembles a string with pearls — such pulsations are called pearls [Guglielmi, Troitskaya, 1973; Fraser et al., 2006; Guglielmi, Potapov, 2019; 2021]. Probably, this term was first used in [Sucksdorff, 1936].

Most of the Pc1-2 ULF waves observed in space are identified with electromagnetic ion cyclotron (EMIC) waves. They are assumed to be generated by ion-cyclotron instability in the near-equatorial region of the magnetosphere due to pressure tensor anisotropy [Cornwall, 1965; Kennel, Petschek, 1966; Guglielmi, 1968]. Theoretical [Horne, Thorne, 1993; Krall, Trivelpiece, 1975] and experimental studies [Young et al., 1981; Anderson et al., 1992b, 1996; Fraser, Nguyen, 2001] have shown that ion-cyclotron waves have left-hand circular polarization. For the ion-cyclotron instability to develop, the wave should be quasi-parallel, i.e. the quasi-parallel wavelength should be much shorter than the perpendicular one.

For a long time, the main model explaining the formation of the Pc1 wave packet was the bouncing wave packet model. According to this model, Pc1 pulsations are wave packets moving along the field line and experiencing periodic reflections from the highly conductive ionosphere [Jacobs, Watanabe, 1964; Obayashi, 1965].

The structure of ion-cyclotron waves across field lines was studied in [Dmitrienko, Mazur, 1992], where it was found that due to the presence of a local minimum in the radial profile of the Alfvén velocity near the plasmapause these waves can be closed into a resonator across magnetic shells in this magnetospheric region.

Later, it turned out that the bouncing wave packet model cannot explain all the Pc1 pulsations observed. On the one hand, satellite data shows that the pearl repetition period is too short to be identified with the period of reflection of the packet from the ionosphere [Mursula et al., 2001; 2007]. On the other hand, in many cases the packet cannot run along the entire field line at all. This is due to the presence of heavy ions in magnetospheric plasma, i.e. ions whose mass is much greater than the mass of protons. Satellite data indicates a high content of oxygen ions in magnetospheric plasma during the magnetic storm recovery phase [Takahashi et al., 2006; Yang et al., 2010]. The importance of taking heavy ions into account for studying Pc1 pulsations was first noted

in [Gintzburg, 1963; Smith, Brice, 1964; Gurnett et al., 1965; Guglielmi, 1967]. Of particular significance is the study of trajectories of ion-cyclotron wave packets in the magnetosphere, carried out in [Rauch, Roux, 1982].

The structure of Pc1 ion-cyclotron waves along the field line in plasma with heavy ions was examined in [Guglielmi et al., 2000, 2001]. The authors showed that such waves can be closed along the field line into a resonator in the equatorial region of the field line. Thus, the packet can oscillate only between boundaries (wave reflection points) of the resonator. These effects were further studied in [Lundin, Guglielmi, 2006; Guglielmi, Kangas, 2007; Guglielmi, Potapov, 2012].

In addition, it was found that in many cases Pc1 pulsations have linear polarization [Young et al., 1981; Anderson et al., 1992b, 1996; Fraser, Nguyen 2001]. Such waves cannot be identified with ion-cyclotron modes, which must be left-hand polarized. Lee et al. [2008] suggested that linearly polarized Pc1 pulsations may be identified with ion-ion hybrid (IIH) waves, which can exist in plasma with the presence of ions of two or more types — lighter and heavier [Buchsbaum, 1960]. In Earth's magnetosphere, it is natural to identify light ions with protons, and heavy ions with oxygen and sometimes helium ions.

In [Mithaiwala et al., 2007; Klimushkin et al., 2010; Farmer, Morales, 2013; Kim et al., 2015a], it has been found that the IIH modes should be closed along the field line into a resonator in the near-equatorial region of the magnetosphere. Indeed, linearly polarized Pc1 pulsations are usually observed near the geomagnetic equator [Anderson et al., 1992a; Horne, Thorne, 1993; Lotoaniu, 2005; Chen et al., 2009]. It is worth noting that theoretically IIH modes arise in the opposite limit compared to ion-cyclotron modes: they should be quasi-perpendicular, i.e. their perpendicular wavelength should be much shorter than the parallel one. The theory of IIH waves in Earth's magnetosphere has been discussed in [Klimushkin et al., 2006, 2010; Mikhailova, 2011; Kazakov and Fulop, 2013; Kim et al., 2015b, 2019; Mikhailova et al., 2020a, b]. Some observed events indicate a strong latitudinal localization of Pc1 waves [Mursula et al., 1994; Engebretson et al., 2002, 2008; Yahnin et al., 2007], which also allows us to associate them with quasi-perpendicular IIH modes. The IIH waves can also exist in Mercury's magnetosphere, where sodium plays the role of heavy ions [Glassmeier et al., 2003, 2004; Kim et al., 2008, 2013].

It is hardly possible to encompass all the available theoretical models explaining the formation mechanisms and the structure of Pc1 pulsations in one review. This paper presents different approaches to the study of short-period ULF waves in a multicomponent plasma: quasi-parallel and quasi-perpendicular approximations. In geophysics, the quasi-parallel approximation usually means wave propagation at an angle not exceeding 45° with respect to the surrounding magnetic field, and the quasi-perpendicular approximation implies wave propagation at an angle from 60° to 90° [Brunelli, Namgaladze, 1988]. From this point on, the term "quasi-parallel" stands for a large value of the parallel wave vector component $k_{\parallel} \to \infty$; and the quasi-perpendicular approximation, a large value of the perpendicular wave vector component $k_{\perp} \to \infty$.

The review has the following structure. Section 1 contains the main equations used for analytical calculations. Section 2 deals with the quasi-parallel approximation used to study the wave structure along field lines (Subsection 2.1) and the spatial structure of ion-cyclotron waves in plasma with heavy ions (Subsection 2.2). Section 3 is devoted to the quasi-perpendicular approximation, the parallel structure of waves in the vicinity of the geomagnetic equator (Subsection 3.2), the possibility of the existence of toroidal and poloidal modes (Subsection 3.3), and the resonator for IIH waves across magnetic shells (Subsection 3.4). Section 4 discusses the localization of waves for an arbitrary wave vector. Section 5 addresses unresolved problems and presents the conclusion.

1. MAIN EQUATIONS

To study ULF waves in a dipole-like magnetosphere, an axially symmetric coordinate system { x^1, x^2, x^3} is used such that the radial coordinate x^1 determines the number of the magnetic shell, the azimuthal coordinate x^2 marks the field line, and parallel coordinate x^3 indicates a point on the field line (Figure 1). We may employ the McIlvaine parameter L as the radial coordinate, and the azimuth angle φ as the azimuthal coordinate. The physical length of a vector in such a coordinate system is determined by the expression $dl_i = \sqrt{g_i}dx^i$. Here, g_i is the metric tensor component, and $\sqrt{g_i}$ is the Lame coefficient. Determinant of the metric tensor: $g = g_1 g_2 g_3$.

In the dipole magnetosphere model, the metric tensor components [Brunelli, Namgaladze, 1988; Leonovich, Mazur, 2016] are expressed through the magnetic latitude θ: $g_1 = \dfrac{\cos^6\theta}{1+3\sin^2\theta}$, $g_2 = L^2\cos^6\theta$. The field line length element can be found as follows

$$dl = \sqrt{g_3}dx^3 = L\cos\theta\sqrt{1+3\sin^2\theta}\,d\theta.$$

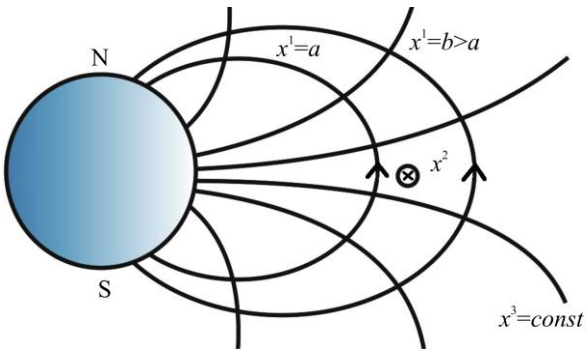

Figure 1. Coordinate system related to the geomagnetic field [Mager, Klimushkin, 2013]

In an axisymmetric magnetic field, all perturbed quantities can be represented as $e^{-i\omega t+ik_2x^2}$, where k_2 is the azimuthal wave vector component. Since the x^2 coordinate is directed along the azimuth, the azimuth angle φ can be used as this coordinate. Then, $k_2=m$, where m is the azimuthal wave number.

Let us consider an ULF wave with a frequency ω propagating in cold plasma consisting of electrons, protons, and heavy ions. Perturbations of the wave electric field $\vec{E}$ can be found from Maxwell equations:

$$\nabla\times\nabla\times\vec{E}=\frac{\omega^2}{c^2}\hat{\varepsilon}\vec{E}, \tag{1}$$

where c is the speed of light; $\hat{\varepsilon}$ is the permittivity tensor. Its components are defined as follows [Glassmeier et al., 2003]:

$$\begin{aligned}&\varepsilon_{\parallel}\to-\infty,\\ &\varepsilon_{\perp}=\frac{\Omega_{pp}^2}{\Omega_{cp}^2-\omega^2}+\frac{\Omega_{ph}^2}{\Omega_{ch}^2-\omega^2},\\ &\eta=\frac{\Omega_{pe}^2}{\omega\Omega_{ce}}-\frac{\Omega_{cp}}{\omega}\frac{\Omega_{pp}^2}{\Omega_{cp}^2-\omega^2}-\frac{\Omega_{ch}}{\omega}\frac{\Omega_{ph}^2}{\Omega_{ch}^2-\omega^2}.\end{aligned} \tag{2}$$

Here, Ω_p and Ω_c are plasma and cyclotron frequencies. The second index denotes the corresponding particle: proton (p); heavy ion (h); electron (e).

In ideal MHD, the wave electric field is a two-dimensional vector (E_1, E_2, 0); the parallel component of the field is zero due to the condition $\varepsilon_{\parallel}\to-\infty$. Assume that across magnetic shells the wave field decreases with distance away from the region under study, giving a boundary condition in x^1

$$\vec{E}\left(x^1\to\infty\right)=\vec{E}\left(x^1\to-\infty\right)=0; \tag{3}$$

in this case, the wave is reflected from the ionosphere due to its high conductivity, which corresponds to the boundary condition in x^3

$$\vec{E}\left(x_-^3\right)=E\left(x_+^3\right)=0, \tag{4}$$

where $x_{\pm}^3$ are the coordinates of the points of intersection of magnetic field lines and the upper boundary of the ionosphere.

In the small-scale approximation, the Wentzel–Kramers–Brillouin (WKB) approximation can be used to study the oscillations, when all perturbed quantities are proportional to $\exp\left(i\int\vec{k}\cdot d\vec{r}\right)$. Then, system (1, 2) reduces to the well-known dispersion equation for ULF waves [Swanson, 2003]:

$$\left(\frac{\omega^2}{c^2}\varepsilon_{\perp}-k_{\parallel}^2\right)\left(\frac{\omega^2}{c^2}\varepsilon_{\perp}-k_{\parallel}^2-k_{\perp}^2\right)=\frac{\omega^4}{c^4}\eta^2, \tag{5}$$

where $k_{\parallel}^2$ and $k_{\perp}^2$ are the wave vector components along and across the magnetic field line.

2. QUASI-PARALLEL APPROXIMATION $k_{\perp}^2/k_{\parallel}^2\to0$

2.1. Parallel resonator

The quasi-parallel approximation for ion-cyclotron waves in plasma with an admixture of heavy ions has been examined in [Guglielmi et al., 2000, 2001; Guglielmi, Potapov, 2012 , 2019]. These papers show the presence of a resonator for ion-cyclotron waves in the equatorial part of the field line. It turned out that in contrast to the bouncing wave packet model the reflection points for a traveling wave packet are located in the vicinity of the geomagnetic equator, not in the ionosphere. It is shown that the wave packet oscillation period in the resonator is approximately equal to the repetition period of elements of Pc1 pulsation series.

Consider a small-scale wave along a magnetic field line. In the quasi-parallel approximation $k_{\perp}^2/k_{\parallel}^2\to0$, dispersion relation (5) takes the form

$$\left(\frac{\omega^2}{c^2}\varepsilon_{\perp}-k_{\parallel}^2\right)^2=\frac{\omega^4}{c^4}\eta^4. \tag{6}$$

This equation has two solutions:

$$k_{\parallel\pm}^2=\frac{\omega^2}{c^2}\left(\varepsilon_{\perp}\pm\eta\right).$$

They refer to left-hand (LH, "+" sign) and right-hand (RH, "–" sign) polarized modes. For a left-hand polarized wave, the function $k_{\parallel}^2\left(x^3\right)$ in the close vicinity of the equator can be represented in the parabolic approximation. We can apply this representation if there are protons and heavy ions in the plasma. The dependence of $k_{\parallel}^2$ on the parallel coordinate along the field line is shown in Figure 2. The value of $k_{\parallel}^2$ is seen to become zero at the reflection points $\pm l_0$, followed by two opaque regions ($k_{\parallel}^2<0$). The concentration of oxygen ions at the equator is much lower than in the near-ionosphere regions. Turning points occur where there are a large number of oxygen ions. The wave is trapped near the equator along the parallel coordinate.

In the vicinity of the equator, the magnetic field B varies slightly and can be represented as

$$B=B_{eq}\left[1+\frac{9}{2}\left(\frac{l}{R_EL}\right)^2\right], \tag{7}$$

where B_{eq} is the geomagnetic field at the equator; $l=\sqrt{g_3}x^3$ is the physical length along the field line; R_EL is the distance from the center of Earth to the top of the field line expressed in Earth radii. The wave structure in the vicinity of the equator can be found from Equation (1). In the quasi-parallel approximation, system of equations (1), along with boundary conditions (4), is an eigenvalue problem for the parameter $k_{\parallel}$ and determines the wave structure along the field line.

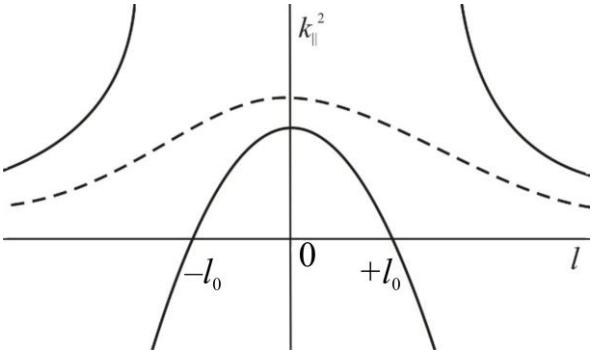

Figure 2. $k_\parallel^2$ as a function of the parallel coordinate l. The solid line indicates the behavior of the function $k_\parallel^2$ for a left-hand polarized wave; the dashed line, for a right-hand polarized wave [Guglielmi et al., 2001]

The parallel wave field structure is described by the parabolic cylinder functions $D_N(\xi)$:

$$D_N\left(\sqrt{2}\xi\right) = He_N(\xi)\exp\left[-\xi^2/2\right], \tag{8}$$

Here, $He_N(\xi)$ are the Hermitian polynomials; N is the parallel wave number. The argument ξ is related to the parallel coordinate by the expression

$$\xi^2 = \frac{3l^2}{\sqrt{2}A_h R_E L}\frac{\Omega_{ch}\Omega_{cp}}{\Omega_{cp}-\Omega_{ch}}\frac{\left(1+\rho_h/\rho_p\right)^{3/2}}{\rho_h/\rho_p}, \tag{9}$$

where $A_{p,h} = B/\sqrt{4\pi\rho_{p,h}}$ is the Alfvén velocity; $\rho_{p,h}$ is the density of protons or heavy ions, depending on the index.

The frequency spectrum of harmonics excited in the ion-cyclotron resonator is equidistant and quantized

$$\omega_N = \left(1+\frac{\rho_h}{\rho_p}\right)\Omega_{ch} + 3\sqrt{2\frac{\rho_h}{\rho_p}}\frac{A_h}{LR_E}\left(N+\frac{1}{2}\right), \tag{10}$$

The frequency spectrum is assumed to be sufficiently dense, i.e. $\Delta\omega = \omega_{N+1}-\omega_N << \omega_{N=0}$. Guglielmi et al. [2001] supposed that the Pc1 pulsations observed are wave packets composed of high N harmonics (N>>1) and running between reflection points of the resonator.

The width of the parallel equatorial resonator is determined by

$$\Delta l = 2\left(\frac{\rho_h}{\rho_p}\right)^{1/4}\left[\frac{A_h R_E L}{\Omega_{ch}}\left(N+\frac{1}{2}\right)\right]^{1/2}, \tag{11}$$

here $\Delta l = 2x_0^3$. For the fundamental harmonic, the size of the resonator is the smallest. For typical parameters of the magnetosphere in the plasmapause region (ρ_h/ρ_p=1.6, A_h=500 km/s, L=5 [Dmitrienko, Mazur, 1992; Yang et al., 2010]), the resonator width is ~1 R_E, the frequency of the fundamental harmonic in the resonator corresponding to the frequency of Pc1 pulsations is ~2.35 Hz.

2.2. Perpendicular resonator

Magnetospheric plasma is inhomogeneous both along field lines and in the radial direction [Leonovich, Mazur, 1993]. The existence of such a region as the plasmapause in the magnetosphere, where a jump occurs in almost all magnetospheric parameters, suggests the existence of a perpendicular resonator for ULF waves in this region, especially since the radial profile of the Alfvén velocity has a local minimum near the plasmapause (Figure 3). The structure of Pc1 oscillations in the resonator formed by a local minimum of the Alfvén velocity has been examined in [Dmitrienko, Mazur, 1985, 1992]; and in the presence of heavy ions in magnetospheric plasma, in [Mikhailova, 2013; Mikhailova, 2014].

Consider an axially symmetric ULF wave (k_2=0). In cold plasma, system of equations (1) can be written as

$$\hat{L}_{ij}E_j = 0. \tag{12}$$

Here, components of the operator $\hat{L}$ look like

$$L_{11} = \frac{\partial}{\partial x^3}\frac{g_2}{\sqrt{g}}\frac{\partial}{\partial x^3} + \frac{\sqrt{g}}{g_1}\frac{\omega^2}{c^2}\varepsilon_\perp, \tag{13}$$

$$\hat{L}_{12} = -i\frac{\omega^2}{c^2}\eta\sqrt{g_3}, \quad \hat{L}_{21} = \hat{L}_{12}^*, \tag{14}$$

$$\hat{L}_{22} = \frac{\partial}{\partial x^1}\frac{g_3}{\sqrt{g}}\frac{\partial}{\partial x^1} + \frac{\partial}{\partial x^3}\frac{g_2}{\sqrt{g}}\frac{\partial}{\partial x^3} + \frac{\sqrt{g}}{g_2}\frac{\omega^2}{c^2}\varepsilon_\perp, \tag{15}$$

the asterisk here denotes complex conjugation. The Hermitian operator is $\hat{L}$.

System (12) will be solved in the WKB approximation as follows

$$E_\alpha = H_\alpha\left(x^1, x^3\right)e^{i\int k_3\left(x^3\right)dx^3},$$

where α is a coordinate; H_α is a function. Equation (12) together with boundary conditions (3) in x^1 represents an eigenvalue problem $k_3 = k_3\left(x^3\right)$. This system contains a derivative only in x^1, hence the function H_α determines the perpendicular structure of the mode.

We deal with the frequency range of the order of the gyrofrequency of heavy ions (much lower than the

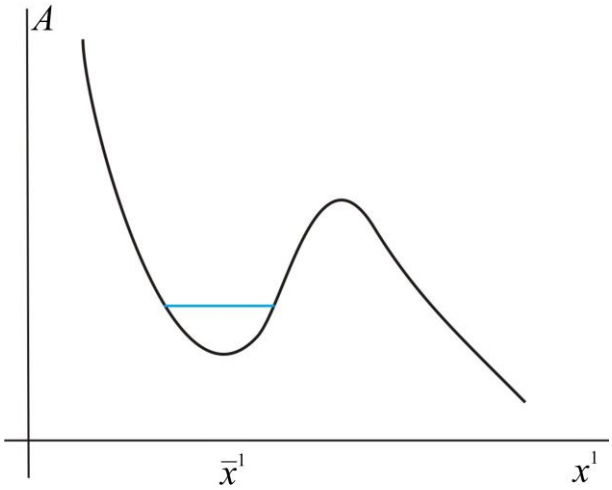

Figure 3. Schematic representation of the radial coordinate dependence of the Alfvén velocity that has a minimum near the plasmapause (blue line) [Mikhailova, 2014]

gyrofrequency of protons). In this case, the diagonal element of the permittivity tensor $\varepsilon_\perp$ can be represented as

$$\varepsilon_\perp \approx \frac{c^2}{A_p^2}\left[1+\frac{A_p^2}{A_h^2\left(1-\frac{\omega^2}{\Omega_{ch}^2}\right)}\right]. \quad (16)$$

Following [Dmitrienko, Mazur, 1992], we examine the region adjacent to the inner edge of the plasmapause, where the radial profile of the Alfvén velocity has a local minimum (see Figure 3). In this case, the function $\varepsilon_\perp$ has a maximum at the plasmapause $(x^1=\bar{x}^1)$ at a fixed value of x^3. When moving away from the plasmapause, $\varepsilon_\perp$ will decrease. In a small neighborhood of the plasmapause, we can use the representation

$$\varepsilon_\perp\left(x^1, x^3\right)=\varepsilon_\perp\left(\bar{x}^1, x^3\right)\left[1-\frac{\left(x^1-\bar{x}^1\right)^2\sqrt{g_1}}{l^{1^2}\left(x^3\right)}\right], \quad (17)$$

where $l^1\left(x^3\right)$ is the scale of the inhomogeneity in x^1. Notice that $l^1\left(x^3\right)=l_\perp\left(x^3\right)/\sqrt{g_1}$, where $l_\perp\left(x^3\right)$ is the scale of the inhomogeneity across magnetic shells. We may ignore variations in the metric tensor coefficients since the region of localization of the wave considered is smaller than the scale of magnetospheric inhomogeneities.

Turn to physical components of the vectors. The wave equation for the perpendicular wave structure takes the form

$$\frac{\partial^2\hat{H}_2^{(0)}}{\partial\xi^2}-\left[\xi^2+k_\parallel'^2\lambda^2-\frac{\tilde{\eta}^2\lambda^2}{\lambda^{-2}\xi^2+k_\parallel'^2}\right]\hat{H}_2^{(0)}=0, \quad (18)$$

here,

$$\lambda^4=\frac{g_1 l_\perp^2 c^2}{\varepsilon_\perp\omega^2}, \quad (19)$$

$$k_\parallel'^2=k_\parallel^2-\frac{\omega^2}{c^2}\varepsilon_\perp, \quad (20)$$

$$\lambda\xi=\hat{x}^1-\hat{\bar{x}}^1, \quad (21)$$

$$\tilde{\eta}=\left(\omega^2/c^2\right)\eta. \quad (22)$$

The turning (reflection) points can be found from $k_1^2=0$. The transparent region $\left(k_1^2>0\right)$ lies between the turning points whose radial coordinates are determined from

$$\hat{x}_0^1=\hat{\bar{x}}^1\pm\left[\frac{g_1 l_\perp^2 c^2}{\varepsilon_\perp\omega^2}\left(\frac{\omega^2}{c^2}\varepsilon_\perp-k_\parallel^2\right)\left(1\pm\sqrt{1+\tilde{\eta}^2}\right)\right]^{1/2}. \quad (23)$$

The resonator is bounded by magnetic shells located at an equal distance from the plasmapause [Dmitrienko, Mazur, 1992]. This fact allows us to consider such a resonator in the same way as potential wells are studied in quantum mechanics. There are two types of potential wells: deep and shallow. The former has a set of discrete energy levels; the latter has one energy level, but has no obvious potential barriers [Landau, Lifshitz, 2004].

Let us take a look at two extreme cases. Given $|\xi|<<\lambda k_\parallel'$ and a new variable $\chi=\sqrt{2}\xi,$, Equation (18) reduces to the equation for parabolic cylinder functions:

$$\frac{\partial^2\hat{H}_2^{(0)}}{\partial\chi^2}-\left[\frac{\chi^2}{4}+\frac{\lambda^2\left(k_\parallel'^4-\tilde{\eta}^2\right)}{2k_\parallel'^2}\right]\hat{H}_2^{(0)}=0, \quad (24)$$

This equation describes a deep potential well. The solution to this equation is a set of eigenfunctions

$$\hat{H}_2^{(0)}=\hat{H}_n^{(0)}=e^{-\xi^2/2}He_n\left(\sqrt{2}\xi\right), \quad (25)$$

with a discrete set of eigenvalues

$$k_{\parallel(n)}'^2=\tilde{\eta}+\frac{1}{\lambda^2}\left(n+\frac{1}{2}\right). \quad (26)$$

Here, the functions He_n are Hermitian polynomials [Abramowitz, Stegun, 1964], n is the perpendicular wave number. Oscillations in such a perpendicular resonator have left-hand circular polarization.

In the opposite case when $\tilde{\eta}<<1$ and $\lambda^2 k_{\parallel(n)}'^2<<1$, Equation (18) takes the form

$$\frac{\partial^2\hat{H}_2^{(0)}}{\partial\xi^2}-\xi^2\hat{H}_2^{(0)}=0. \quad (27)$$

This is another equation for the parabolic cylinder functions — an equation for a shallow well, which has a single eigenfunction

$$\hat{H}_2^{(0)}=CD_{-1/2}\left(\sqrt{2}\xi\right), \quad (28)$$

where C is the constant; $D_n(\xi)$ is the Whittaker function [Abramowitz, Stegun, 1964]. The only eigenvalue of the shallow well problem has the form [Landau, Lifshitz, 2004]

$$k_\parallel'^2=\frac{\pi^2}{8}\frac{\Gamma^2\left(1/4\right)}{\Gamma^2\left(3/4\right)}\tilde{\eta}^4\lambda^6. \quad (29)$$

The shallow well contains only one harmonic, which is a surface wave whose tails extend beyond the resonator.

The frequency spectrum of oscillations in the resonator of the deep potential well type can be obtained using the Bohr-Sommerfeld condition of quantization

$$\int_{-l_0}^{l_0}k_\parallel^{(n)}\left(l'\right)dl'=\pi\left(N+\frac{1}{2}\right), \quad (30)$$

where n and N are the perpendicular and parallel quantum numbers respectively. We can use the Bohr-Sommerfeld condition of quantization for large values of N, but, as practice shows, this condition yields the correct result even for values of the parallel wave number of the order of unity. Since $k_\parallel\left(l,\omega_{nN}\right)$ depends on the frequency $\omega=\omega_{nN}$ as a parameter, we can get the wave frequency. From Equation (26) we derive the parallel component of the wave vector

$$k_\parallel^{(n)2}=\frac{\omega^2}{c^2}\varepsilon_\perp+\frac{\omega^2}{c^2}\eta+\frac{\omega\sqrt{\varepsilon_\perp}}{cl_\perp\sqrt{g_1}}\left(n+\frac{1}{2}\right). \quad (31)$$

Using quantization condition (30), we can obtain an expression for the frequency

$$\omega_{nN}=\left(1+\frac{\rho_h}{\rho_p}\right)\Omega_{ch}+3\sqrt{2\frac{\rho_h}{\rho_p}}\frac{A}{R_E L}\left(N+\frac{1}{2}\right)+ \\ +3\sqrt{\frac{\rho_h}{2\rho_p}}\left(2+\frac{\rho_h}{\rho_p}\right)^{-3/4}\frac{A^2}{\Omega_{ch}l_\perp R_E L}\left(N+\frac{1}{2}\right)\left(n+\frac{1}{2}\right), \quad (32)$$

where $A=B/\sqrt{4\pi\left(\rho_p+\rho_h\right)}$ is the Alfvén velocity. Here, magnetic field inhomogeneity along field line (7) is taken into account.

Make numerical estimates for the main harmonic (N=0, n=0). For this purpose, as above, we use the parameter values typical for the magnetosphere in the plasmapause region: ρ_h/ρ_p=1.6, A=500 km/s, L=5, $\Omega_{ch}\approx 1$ s^{-1}, $l_\perp\sim 10^4$ km [Dmitrienko, Mazur, 1992; Yang et al., 2010]. The frequency of the main harmonic is ω_0=2.64 s^{-1}, the turning points along and across the field line are at a distance of $\sim 1\ R_E$ from the equator and the center of the plasmapause. The opaque regions are assumed to be sufficiently wide, so we can neglect the wave energy leakage to the ionosphere.

Spectrum (32) partially coincides with spectrum (10) obtained in [Guglielmi et al., 2000]. The fundamental difference is in the last term of Expression (32). This term takes into account the perpendicular wave structure; the wave frequency depends on parallel N and perpendicular n wave numbers, while Expression (10) includes the dependence only on the parallel structure.

3. QUASI-PERPENDICULAR APPROXIMATION $k_\parallel/k_\perp\to 0$

3.1. Two modes of ion-ion hybrid waves

Examine the ULF-wave structure in the quasi-perpendicular approximation. To study waves in plasma, it is convenient to use the method proposed in [Tamao, 1984; Klimushkin, 1994]. Since the parallel wave electric field is considered to be negligible, the electric field vector can be expressed as the sum of potential and vortex components, each is expressed through a scalar function — potential (note that this term is used here in a slightly different sense than in standard textbooks on electrodynamics)

$$\vec{E}=-\nabla_\perp\Phi+\nabla_\perp\times\vec{e}_\parallel\Psi. \quad (33)$$

Here, $\vec{e}_\parallel=\vec{B}/B$, $\nabla_\perp$ is the two-dimensional nabla operator in a plane (x^1, x^2). In a homogeneous plasma in the $\omega/\Omega_c\to 0$ approximation, the potentials Φ and Ψ are the Alfvén wave and the fast magnetic sound respectively [Tamao, 1984; Klimushkin, 1994]. In the general case, the wave determined by the potential Φ is called the guided mode, i.e. propagating along the equilibrium magnetic field (directed by it); and that defined by Ψ, the isotropic mode. Linearly polarized quasi-perpendicular waves can be interpreted as ion-ion hybrid (IIH) waves. In terms of the Φ potential, they are guided modes in multi-ion plasma.

System of equations (1) after some algebraic transformations turns into a system of equations for Φ and Ψ

$$\left[\partial_1\hat{L}_T\partial_1+\partial_2\hat{L}_P\partial_2\right]\Phi- \\ -i\frac{\omega^2}{c^2}\left[\partial_1\sqrt{g_3}\eta\partial_2-\partial_2\sqrt{g_3}\eta\partial_1\right]\Phi= \\ =i\frac{\omega^2}{c^2}\left[\partial_1\sqrt{\frac{g_2}{g_1}}\eta\partial_1+\partial_2\sqrt{\frac{g_1}{g_2}}\eta\partial_2\right]\Psi+ \\ +\left[\partial_1\hat{L}_T\frac{g_1}{\sqrt{g}}\partial_2-\partial_2\hat{L}_P\frac{g_2}{\sqrt{g}}\partial_1\right]\Psi, \quad (34)$$

$$\Delta_\perp\frac{g_3}{\sqrt{g}}\Delta_\perp\Psi+ \\ +\left[\partial_1\frac{g_2}{\sqrt{g}}\hat{L}_T\frac{g_2}{\sqrt{g}}\partial_1+\partial_2\frac{g_1}{\sqrt{g}}\hat{L}_P\frac{g_1}{\sqrt{g}}\partial_2\right]\Psi- \\ -i\frac{\omega^2}{c^2}\left[\partial_1\frac{\eta}{\sqrt{g_3}}\partial_2-\partial_2\frac{\eta}{\sqrt{g_3}}\partial_1\right]\Psi= \quad (35) \\ =-i\frac{\omega^2}{c^2}\left[\partial_1\sqrt{\frac{g_2}{g_1}}\eta\partial_1+\partial_2\sqrt{\frac{g_1}{g_2}}\eta\partial_2\right]\Phi+ \\ +\left[\partial_2\frac{g_1}{\sqrt{g}}\hat{L}_T\partial_1-\partial_1\frac{g_2}{\sqrt{g}}\hat{L}_P\partial_2\right]\Phi.$$

The operators introduced here

$$\hat{L}_T(\omega)=\partial_3\frac{g_2}{\sqrt{g}}\partial_3+\frac{\sqrt{g}}{g_1}\varepsilon_\perp\frac{\omega^2}{c^2}, \quad (36)$$

$$\hat{L}_P(\omega)=\partial_3\frac{g_1}{\sqrt{g}}\partial_3+\frac{\sqrt{g}}{g_2}\varepsilon_\perp\frac{\omega^2}{c^2} \quad (37)$$

are called toroidal and poloidal operators, and $\Delta_\perp\equiv\partial_1\left(g_2/\sqrt{g}\right)\partial_1+\partial_2\left(g_1/\sqrt{g}\right)\partial_2$ is a perpendicular Laplace operator. If instead of x^3 we enter the parallel coordinate $\left(dl=\sqrt{g_3}dx^3\right)$, the operators will take the form

$$\hat{L}_T(\omega)=\sqrt{g_3}\left(\frac{\partial}{\partial l}\sqrt{\frac{g_2}{g_1}}\frac{\partial}{\partial l}+\sqrt{\frac{g_2}{g_1}}\frac{\omega^2}{c^2}\varepsilon_\perp\right), \quad (38)$$

$$\hat{L}_P(\omega)=\sqrt{g_3}\left(\frac{\partial}{\partial l}\sqrt{\frac{g_1}{g_2}}\frac{\partial}{\partial l}+\sqrt{\frac{g_1}{g_2}}\frac{\omega^2}{c^2}\varepsilon_\perp\right). \quad (39)$$

Deriving $\Delta_\perp\Psi$ from (35) and substituting it in (34), we can reduce the system to a single equation

$$\partial_1\hat{L}_T(\omega)\partial_1\Phi+\partial_2\hat{L}_P(\omega)\partial_2\Phi- \\ -\sqrt{g}\left(\frac{\omega^2}{c^2}\eta\right)^2\Phi=0. \quad (40)$$

We deal with small-scale inhomogeneous oscillations across field lines and in the azimuthal direction; therefore, in the quasi-perpendicular approximation the third term on the left side of (40) is much smaller than the others. Then the wave equation for IIH modes takes the

form [Klimushkin et al., 2010]

$$\partial_1 \hat{L}_T(\omega)\partial_1\Phi + \partial_2 \hat{L}_P(\omega)\partial_2\Phi = 0. \quad (41)$$

Let us take a look at two extreme cases. In the first, the radial wavelength λ_r is much smaller than the azimuthal one λ_a. This means that the radial component of the electric field is much larger than the azimuthal component $E_r >> E_a$ in one case, and $E_a >> E_r$ in the other.

In the first case when the first term of Equation (41) dominates over the second, the wave function Φ is proportional to the eigenfunction of the toroidal operator T_N

$$\hat{L}_T(\omega)T_N(x^3) = 0; \quad (42)$$

the boundary conditions of the problem are given in the form $T_N(x_\pm^3) = 0$, which follows from boundary condition (4); the points $x_\pm^3$ are the coordinates of intersection of the field line and the ionosphere. The number N denotes the parallel wave number. The eigenvalue Ω_{TN} is called the toroidal eigenfrequency. Thus, if the wave frequency ω coincides with the toroidal natural frequency Ω_{TN}, its structure along the field line is described by the toroidal eigenfunction $T_N(x^3)$; such a wave has toroidal polarization: $E_r >> E_a$ or $B_a >> B_r$. The IIH wave with this polarization is known as the toroidal IIH mode.

In the other extreme case when $\lambda_r >> \lambda_a$, the wave has poloidal polarization: $E_a >> E_r$. In this case, in Equation (41) the second term is dominant and the function Φ should be proportional to the poloidal eigenfunction P_N:

$$\hat{L}_P(\omega)P_N(x^3) = 0; \quad (43)$$

boundary functions are chosen similarly to the previous case $P_N(x_\pm^3) = 0$. If the wave frequency ω coincides with the eigenvalue of the problem (poloidal frequency Ω_{PN}), the parallel structure of the wave is described by the poloidal eigenfunction $P_N(x^3)$, and such an IIH wave is referred to as poloidal IIH mode, or IIH wave with poloidal polarization ($B_r >> B_a$).

The magnetic field of a wave can be found from the Faraday law $\nabla \times \vec{E} = \frac{i\omega}{c}\vec{B}$. In terms of potentials, the Φ and Ψ magnetic field components are written as follows:

$$B_{1,2} = \pm\frac{ic}{\omega}\frac{g_{1,2}}{\sqrt{g}}\left(\partial_{2,1}\partial_3\Phi \pm \partial_3\frac{g_{2,1}}{\sqrt{g}}\partial_{1,2}\Psi\right), \quad (44)$$

$$B_3 = \frac{ic}{\omega}\frac{g_3}{\sqrt{g}}\triangle_\perp\Psi. \quad (45)$$

3.2. Parallel resonator

While the operators $\hat{L}_T$ and $\hat{L}_P$ are different and Equations (42), (43) have different eigenfunctions, the squared parallel wave vector component $k_\parallel^2 = k_3^2/g_3$ in the parallel WKB approximation is the same for both modes:

$$k_\parallel^2 = \frac{\omega^2}{A_p^2\left(1-\frac{\omega^2}{\Omega_{cp}^2}\right)} + \frac{\omega^2}{A_h^2\left(1-\frac{\omega^2}{\Omega_{ch}^2}\right)}. \quad (46)$$

Here, $A_{p,h}$ are the Alfvén velocities defined for protons and heavy ions $A_{p,h} = \frac{B_0}{\sqrt{4\pi n_{p,h} m_{p,h}}}$, where $n_{p,h}$ and $m_{p,h}$ are concentrations and masses of protons and heavy ions.

We examine modes with a frequency below the proton gyrofrequency Ω_{cp}. The magnetic field strength is low at the equator and much higher near the ionosphere. We can find a point on the field line, where the wave frequency coincides with the gyrofrequency of heavy ions $\omega=\Omega_{ch}$ (Figure 4). Call this point the singular point l_s. At this point $|k_\parallel|^2 \to \infty$, and on the equatorial side of this point $k_\parallel^2 < 0$. At the equator, the value of Ω_{ch} is small, and it is possible here that $k_\parallel^2 > 0$. Therefore, somewhere between the equator and the singular point there should be a point where $k_\parallel^2 = 0$, — let us call it the turning point l_0. Position of the turning point can be found from $\omega = \Omega_0(l)$, where Ω_0 is the reflection frequency,

$$\Omega_0^2 = \Omega_{ch}^2\left(1+\frac{\rho_h}{\rho_p}\right), \quad (47)$$

recall that $\rho_{h,p} = n_{h,p}m_{h,p}$ are densities of heavy ions and protons [Klimushkin et al., 2006].

In the quasi-perpendicular approximation, as well as in the quasi-parallel one, in the vicinity of the equator there is a resonator where oscillations are generated. It is bounded on both sides by turning points $\pm l_0$ (north–south symmetry). Outside the equatorial resonator there are two opaque regions ending in singular points. Farther, there are transparent regions bordering on the ionosphere of the Northern and Southern hemispheres.

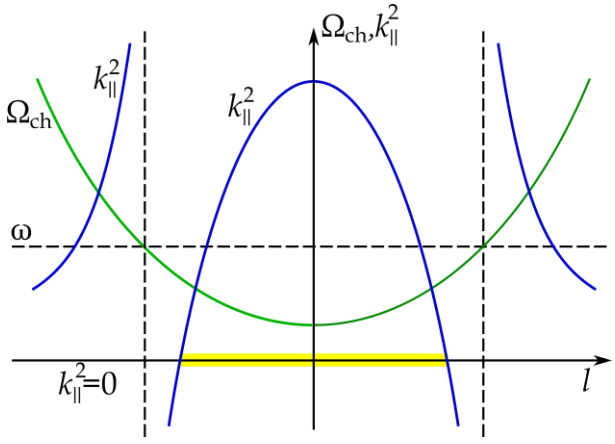

Figure 4. Behavior of the functions $\Omega_{ch}(l)$ (green line) and $k_\parallel^2(l)$ (blue line) along a field line. The equatorial resonator is highlighted in yellow [Mikhailova et al., 2020a]

The equatorial resonator works as a reservoir of energy for waves. The eigenfrequencies of the resonator determine frequencies of the harmonics excited in it.

Near the equator, $k_\parallel^2(l)$ has a maximum and can be represented as expansion

$$k_\parallel^2(\omega, l) = k_{\parallel eq}^2 + \frac{1}{2}\frac{\partial^2\left(k_\parallel^2\right)}{\partial l^2}\bigg|_{eq} l^2, \quad (48)$$

the value is taken at the equator. The turning point is determined from $l_0(\omega_N) = \sqrt{-2k_{\parallel eq}^2 / \left(k_{\parallel eq}^2\right)''}$. The eigenfrequency ω_N, where N is the parallel wave number, can be derived from the Bohr-Sommerfeld condition of quantization

$$\omega_N^2 = \left(1+\frac{\rho_h}{\rho_p}\right)\Omega_{ch}^2 + (2N+1)\frac{\rho_h}{\rho_p}\frac{A_h\Omega_{ch}}{r_{eq}}, \quad (49)$$

where r_{eq} is the equatorial radius of field line curvature. All variables depending on l are taken in their equatorial values $\left(\Omega_{ch}, A_{h,p}, \rho_{h,p}\right)$. The prime means differentiation along the parallel coordinate $(...)' = \partial(...)/\partial l$. It is assumed here that the resonator is well separated from the transparent regions that are located near the ionosphere. In this case, the near-ionospheric transparent regions introduce exponentially small corrections to the resonator's eigenfrequencies [Klimushkin et al., 2010].

The ratio of the first term from (49) to the second $\sim a\Omega_{ch}/A_h >> 1$, therefore the mode frequency is largely determined by the first term (here a is the field line length) and coincides with the equatorial value of the parallel reflection frequency obtained in (47). The frequency spectrum is very dense: $|\omega_{N+1} - \omega_N| << \omega_N$. Simultaneously, all natural harmonics of the resonator are excited which leads to the formation of beats characteristic of Pc1 pearls.

The resonator half-width is written as

$$l_0 \approx r_{eq}\sqrt{\frac{(2N+1)}{\left(1+\rho_p/\rho_h\right)}\frac{A_h}{\Omega_{ch} r_{eq}}}, \quad (50)$$

and the singular point,

$$l_s \approx r_{eq}\sqrt{2}\left[\left(1+\rho_h/\rho_p\right)^{1/2} - 1\right]^{1/2}. \quad (51)$$

Make some quantitative estimates. Assuming that the main admixture of heavy ions in magnetospheric plasma is oxygen O^+ and taking A_h=A_p=10^3 km/s, L=6.6, for the fundamental harmonic (n=0) we get: $\omega_0 \approx 0.875$ rad/s, $l_0 \approx 0.23 r_{eq} = 0.5 R_E$, and $L_s = 0.9 r_{eq}$. The frequency derived is included in the Pc1 frequency range and coincides in order of magnitude with the results obtained in [Guglielmi et al., 2000, 2001; Guglielmi and Kangas, 2007].

3.3. Equatorial modes

Since the mode is trapped in the equatorial resonator, we can consider all values in a small neighborhood of the equator. The angle θ (geomagnetic latitude) can be expanded near the equator

$$\theta(l) = \theta(0) + \theta'(0) l. \quad (52)$$

At the equator, θ(0)=0. Denote the parallel wave vector component $k_\parallel$ for convenience by the letter κ, and in the vicinity of the equator it takes the form

$$\kappa^2 = \frac{\omega^2}{A_{h_{eq}}^2}\left[\frac{\rho_{p_{eq}}}{\rho_{h_{eq}}} + \left(1-\frac{\omega^2}{\Omega_{ch_{eq}}^2}\right)^{-1} - \frac{9\omega^2}{\Omega_{ch_{eq}}^2}\left(1-\frac{\omega^2}{\Omega_{ch_{eq}}^2}\right)^{-2}\frac{l^2}{L^2}\right], \quad (53)$$

Equation (41) is transformed as follows:

$$L^2\frac{\partial}{\partial L}\hat{\mathcal{L}}_T(\omega)\frac{\partial}{\partial L}\Phi(L,l) - m^2\hat{\mathcal{L}}_P(\omega)\Phi(L,l) = 0, \quad (54)$$

where $\hat{\mathcal{L}}_T$ and $\hat{\mathcal{L}}_p$ are the toroidal and poloidal operators, which in the equatorial approximation take the form

$$\hat{\mathcal{L}}_T(\omega) = \frac{\partial^2}{\partial l^2} + \frac{3l}{L^2}\frac{\partial}{\partial l} + \frac{\omega^2}{A_h^2}\left[\frac{\rho_p}{\rho_h} + \left(1-\frac{\omega^2}{\Omega_{ch}^2}\right)^{-1} - \frac{9\omega^2}{\Omega_{ch}^2}\left(1-\frac{\omega^2}{\Omega_{ch}^2}\right)^{-2}\frac{l^2}{L^2}\right], \quad (55)$$

$$\hat{\mathcal{L}}_p(\omega) = \frac{\partial^2}{\partial l^2} - \frac{3l}{L^2}\frac{\partial}{\partial l} + \frac{\omega^2}{A_h^2}\left[\frac{\rho_p}{\rho_h} + \left(1-\frac{\omega^2}{\Omega_{ch}^2}\right)^{-1} - \frac{9\omega^2}{\Omega_{ch}^2}\left(1-\frac{\omega^2}{\Omega_{ch}^2}\right)^{-2}\frac{l^2}{L^2}\right], \quad (56)$$

The difference between the operators is in the sign of the term with the first derivative.

Equation for toroidal eigenfunctions (42) in the equatorial approximation is transformed as follows:

$$\frac{\partial^2}{\partial l^2}T + \frac{3l}{L^2}\frac{\partial}{\partial l}T + \kappa^2 T + \frac{1}{2}\frac{\partial^2\kappa^2}{\partial l^2}l^2 T = 0. \quad (57)$$

This equation reduces to the Hermite equation, whose solution is the toroidal eigenfunction

$$T_N = C\pi^{-1/4}2^{-N/2}(N!)^{-1/2}e^{-\frac{1}{2}\left(\alpha+\lambda^{-2}\right)l^2}He_N\left(\frac{l}{\lambda}\right), \quad (58)$$

where C is the arbitrary constant, $\lambda = \left(\alpha^2+\gamma\right)^{-1/4}$, $\alpha = \frac{3}{2L^2}$, $\gamma = -\frac{1}{2}\frac{\partial^2\kappa^2}{\partial l^2} > 0$, λ is the characteristic wavelength in the resonator. The fundamental harmonic has a wave number N=0.

The spectrum of toroidal eigenfrequencies is written by the equation

$$\Omega_{TN}^2 = 2\Omega_{ch}^2\frac{\rho_h}{\rho_p}(3N+2) + \frac{3A_p^2}{L^2}(N+1). \quad (59)$$

In a similar way, we seek the parallel structure of the poloidal mode. Write equation for the poloidal eigen-

function (43) with poloidal operator (56) in explicit form

$$\frac{\partial^2}{\partial l^2}P-\frac{3l}{L^2}\frac{\partial}{\partial l}P+\kappa^2 P+\frac{1}{2}\frac{\partial^2\kappa^2}{\partial l^2}l^2P=0. \quad (60)$$

The solution to Equation (60) is as follows:

$$P_N=C\pi^{-1/4}2^{-N/2}\left(N!\right)^{-1/2}e^{\frac{1}{2}\left(\alpha-\lambda^{-2}\right)l^2}He_N\left(\frac{l}{\lambda}\right). \quad (61)$$

The structure of the toroidal and poloidal eigenfunctions (fundamental harmonic) is shown in Figure 5. The profile of the poloidal mode is seen to be wider than that of the toroidal mode.

The spectrum of poloidal eigenfrequencies is written as

$$\Omega_{PN}^2=2\Omega_{ch}^2\frac{\rho_h}{\rho_p}\left(3N+2\right)+\frac{3NA_p^2}{L^2}. \quad (62)$$

The obtained value is higher than the gyrofrequency of heavy ions, but lower than toroidal eigenfrequency (59). Thus, the spectrum of IIH waves in the magnetosphere features polarization splitting, similarly to the spectrum of Alfvén waves. However, unlike Alfvén waves, the field line oscillates only in the equatorial part (Figure 6). The parallel structure of the first three IIH-wave harmonics is schematically shown in Figure 7. Eigenfrequencies are related by

$$\Delta\Omega_N^2=\Omega_{TN}^2-\Omega_{PN}^2=\frac{3}{L^2}A_p^2. \quad (63)$$

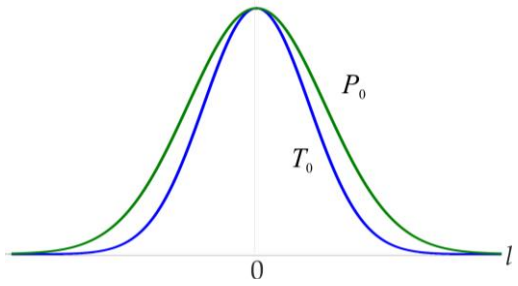

Figure 5. Fundamental harmonics of toroidal and poloidal eigenfunctions (N=0) [Mikhailova et al., 2020a]

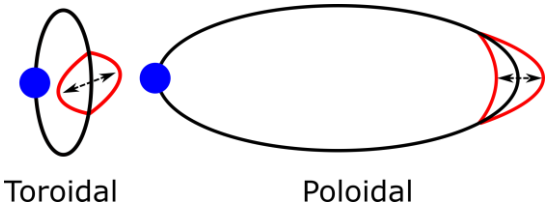

Figure 6. Toroidal and poloidal IIH waves [Mikhailova et al., 2020a]

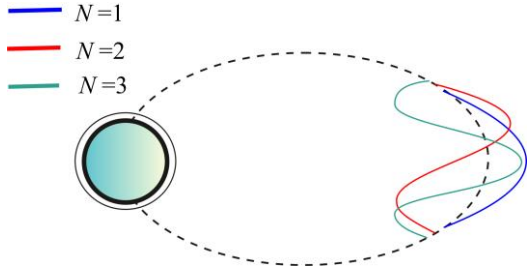

Figure 7. Parallel structure of the first three IIH-wave harmonics in the equatorial resonator

Relative difference

$$\frac{\Delta\Omega^2}{\Omega_{T0}^2}=\frac{\Delta\Omega^2}{\Omega_{P0}^2}=\frac{3A_p^2\rho_p}{4\Omega_{ch}^2L^2\rho_h}. \quad (64)$$

Given the values of the magnetospheric parameters $\rho_p\sim\rho_h$ and $A_p\sim10^3$ km/s, in the geostationary orbit (L=6.6 R_E) we get $\Delta\Omega^2/\Omega_{T0}^2\sim10^{-3}$.

3.4. Perpendicular resonator

The poloidal eigenfrequency of IIH wave $\Omega_{PN}(L)$ changes slowly along the radial coordinate L if the density ratio ρ_h/ρ_p is constant. It can be seen from (62) that $\Omega_{PN}^2(L)$ can have a local minimum in two cases. First, if ρ_h changes more slowly than ρ_p, the behavior of $\Omega_{PN}(L)$ repeats the behavior of the Alfvén velocity function, which has a minimum at the plasmapause. Second, the poloidal frequency has a minimum when ρ_h has a local minimum. In both cases, near the local minimum of $\Omega_{PN}^2(L)$ a perpendicular resonator bounded by two reflection points can be formed (Figure 8) [Mikhailova et al., 2020b].

Since the perpendicular resonator is bounded by poloidal reflection surfaces, the first term of Equation (54) is smaller than the second, which implies that the wave frequency in the resonator is closer to the poloidal frequency Ω_{PN} and its parallel structure is approximately described by the poloidal eigenfunction PN. In this case, the solution of Equation (54) can be sought as follows

$$\Phi=f(L)P_N(l,L)+\delta\Phi, \quad (65)$$

where $f(L)$ is an undetermined function, and $\delta\Phi$ is adjustment of the finite but small value of the first term from Equation (54), which we have ignored: $|\delta\Phi|<<|\Phi|$. Accordingly, the wave frequency can be represented as

$$\omega^2=\Omega_{PN}^2+\left(\omega^2-\Omega_{PN}^2\right), \quad (66)$$

it is assumed here that $\left|\omega^2-\Omega_{PN}^2\right|<<\Omega_{PN}^2$. In view of this, Equation (54) is transformed into

$$\frac{\partial^2 f}{\partial L^2}+\frac{m^2}{6A_h^2}\left[\frac{\rho_p}{\rho_h}+\frac{1}{\left(1-\frac{\Omega_{PN}^2}{\Omega_{ch}^2}\right)^2}\right]\left(\omega^2-\Omega_{PN}^2\right)f- \quad (67)$$
$$-\frac{3m^2}{L^2A_h^2}\frac{\Omega_{PN}^2\left(\omega^2-\Omega_{PN}^2\right)}{\Omega_{ch}^2\left(1-\frac{\Omega_{PN}^2}{\Omega_{ch}^2}\right)^3}\lambda^2Jf=0.$$

Here, $J=\frac{\partial}{\partial\mu}\ln I$, where $\mu=\alpha\lambda^2$,

$$I=\frac{\mu^N}{(1-\mu)^{N+\frac{1}{2}}}\,{}_2F_1\left(-N,-N;\frac{1}{2}-N;\frac{1-\mu}{1-2\mu}\right),$$

and ${}_2F_1$ is the hypergeometric function.

In the vicinity of the local minimum of the function

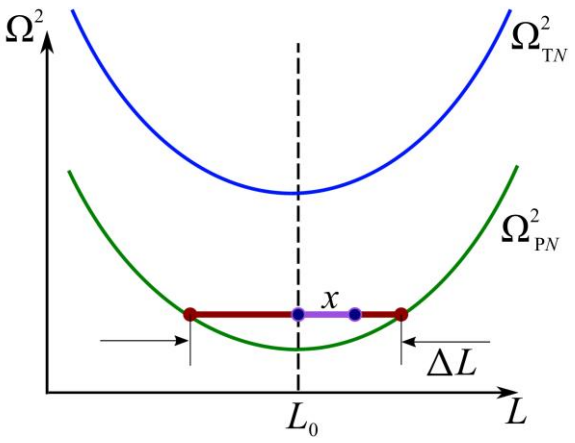

Figure 8. Ω_{TN}^2 and Ω_{PN}^2 as a function of the radial coordinate L [Mikhailova et al., 2020b]

$\Omega_{PN}^2(L)$, this function can be represented as

$$\Omega_{PN}^2(L)=\Omega_{PN}^2(L_0)\left[1+\left(\frac{x}{l_\perp}\right)^2\right], \tag{68}$$

where $l_\perp$ is the perpendicular scale of the inhomogeneity ($l_\perp\sim1\ R_E$), $x=L-L_0$ is the distance from the minimum point of L_0. Values of A_h, $\frac{\Omega_{PN}^2}{\Omega_{ch}^2}$, $\frac{\rho_p}{\rho_h}$ and $\frac{\mu}{\alpha}$ should be taken at L_0. Then, Equation (67) takes the form

$$\frac{\partial^2 f}{\partial L^2}+\frac{m^2}{6A_h^2}\varrho\left(\omega^2-\Omega_{PN}^2\left[1+\left(\frac{x}{l_\perp}\right)^2\right]\right)f=0, \tag{69}$$

where

$$\varrho=\frac{\rho_p}{\rho_h}+\left(1-\frac{\Omega_{PN}^2}{\Omega_{ch}^2}\right)^{-2}-\frac{18\lambda^2 J}{L_0^2}\frac{\Omega_{PN}^2}{\Omega_{ch}^2}\left(1-\frac{\Omega_{PN}^2}{\Omega_{ch}^2}\right)^{-3}.$$

Let us introduce a new variable $\xi=\zeta x$, where $\zeta^2=\frac{m\Omega_{PN}\sqrt{\varrho}}{\sqrt{6}l_\perp A_h}$, then Equation (69) can be reduced to the Hermite equation

$$f''(\xi)-\left(\sigma-\xi^2\right)f(\xi)=0. \tag{70}$$

Here,

$$\sigma=\frac{ml_\perp\sqrt{\varrho}}{\sqrt{6}A_h}\frac{\omega^2-\Omega_{PN}^2}{\Omega_{PN}}.$$

The solution of Equation (70) is written as

$$f_n(\xi)=\pi^{-1/4}2^{-n/2}(n!)^{-1/2}He_n(\xi)e^{-\xi^2/2}. \tag{71}$$

Spectrum of wave oscillations in a perpendicular poloidal resonator

$$\omega_{nN}^2=\Omega_{PN}^2+\frac{\sqrt{6}A_h\Omega_{PN}}{ml_\perp\sqrt{\varrho}}(2n+1). \tag{72}$$

Coordinates of the reflection surfaces bounding the resonator can be found from

$$L_{turn}=L_0\pm l_\perp\frac{\sqrt{\omega^2-\Omega_{PN}^2}}{\Omega_{PN}}, \tag{73}$$

The width of the perpendicular resonator ΔL depends on the azimuthal wave number m

$$\triangle L(m)=2\sqrt{\frac{\sqrt{6}A_h l_\perp}{m\Omega_{PN}\sqrt{\varrho}}(2n+1)}.` \tag{74}$$

Ultimately, the expression for the wave field looks like:

$$\Phi_{Nn}=const\,He_N(l/\lambda)\times \\ \times He_n(\zeta x)e^{\frac{1}{2}\left[\left(\alpha-\lambda^{-2}\right)l^2-\zeta^2x^2\right]}e^{im\varphi-i\omega t}. \tag{75}$$

The wave running in the azimuth direction is localized in the radial direction and along the field line in the vicinity of the geomagnetic equator. Write down the structure of the fundamental harmonic (N=0, n=0)

$$\Phi_{00}=const\,e^{\frac{1}{2}\left[\left(\alpha-\lambda^{-2}\right)l^2-\zeta^2x^2\right]}e^{im\varphi-i\omega t}. \tag{76}$$

Let us present some estimates of the eigenfrequency and width of the resonator with the fundamental harmonic. Use the values typical for the magnetosphere: A_p=1000 km/s, $l_\perp=1R_E$, $L_0=5R_E$, Ω_{ch}=0.67 s^{-1}. We consider oxygen ions as heavy ions, hence the ratio of densities ρ_h/ρ_p=1.6 [Yang et al., 2010]. For the azimuthal wave number m=10, the wave frequency $\omega\approx1.7$ rad/s (~ 0.3 Hz). This value falls within the Pc1 wave frequency range. The width of the perpendicular resonator $\Delta L\approx0$ .3 R_E, its small dimensions agree with the results of observations of Pc1 waves in space [Mursula et al., 1994]. The structure of the fundamental harmonic calculated for these parameters is shown in Figure 9. Thus, we can assume that some of the Pc1 pulsations observed can be interpreted as IIH waves trapped in the perpendicular resonator.

The perpendicular resonator for IIH waves can be formed in the region of the local minimum of $\Omega_{PN}(x^1)$. This is possible near the plasmapause and in the region where there is a jump in plasma parameters and the function ρ_h has a local minimum. A wave in such a resonator will have predominantly poloidal polarization; such poloidal resonators are likely to be observed already [Yeoman et al., 2012; Mager et al., 2018; Polyakov, 2019].

An important difference between IIH waves and Alfvén waves is the presence of a large component of

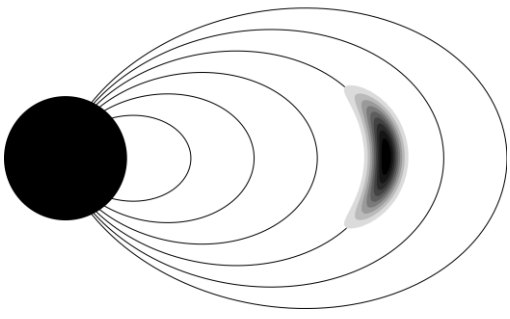

Figure 9. Amplitude distribution of the fundamental harmonic in the coordinates $\{x^1, x^3\}$ [Mikhailova et al., 2020b]

the parallel magnetic field $B_\parallel$. In a homogeneous plasma, Alfvén waves do not have a parallel (compression) component, but it can be significant in a hot plasma with a curved magnetic field [Southwood, Saunders, 1985; Klimushkin and Mager, 2015]. IIH waves, in turn, have a large compression component of the magnetic field even in a homogeneous plasma. Recall the system of equations for the magnetic field in terms of the potentials Φ and Ψ:

$$B_{1,2} = \mp \frac{ic}{\omega} \frac{g_{1,2}}{\sqrt{g}} \left(\partial_{2,1} \partial_3 \Phi \pm \partial_3 \frac{g_{2,1}}{\sqrt{g}} \partial_{1,2} \Psi \right), \quad (77)$$

$$B_3 = \frac{ic}{\omega} \frac{g_3}{\sqrt{g}} \Delta_\perp \Psi. \quad (78)$$

From Equation (78), in view of (35), we can obtain an expression for $B_\parallel$ for IIH waves:

$$B_\parallel = \frac{\omega}{c} \eta \Phi. \quad (79)$$

Deriving Φ from $B_\perp$ and using (77), we can get the ratio of the parallel component of the magnetic field to the perpendicular one. For example, for the poloidal mode this ratio has the form

$$\frac{B_\parallel}{B_r} = \frac{1}{m} \frac{\Omega_{ch}^2 L^2}{A_h^2}. \quad (80)$$

This ratio depends on the azimuthal number m, but it is obvious that the parallel component of the field $B_\parallel$ may be much larger than the perpendicular one. This effect has already been observed for IIH waves of the planet Mercury [Glassmeier et al., 2003].

4. REGION OF RESONATOR LOCALIZATION AT AN ARBITRARY PERPENDICULAR WAVE VECTOR

It follows from the above that both ion-cyclotron and IIH waves feature the parallel resonator near the equator, although dimensions of the resonator, i.e. position of the reflection points, are different. Mathematically, these waves differ in that they have different relationships between perpendicular and parallel wave vector components: in the former case $k_\parallel >> k_\perp$, in the latter $k_\parallel << k_\perp$. In fact, these are two special cases of the same wave. It is likely that in one spatial region the wave exhibits signs of an ion-cyclotron quasi-parallel wave, while in another region the wave is quasi-perpendicular and has linear polarization. When excited by a monochromatic source, the wave can be transformed from the ion cyclotron mode to the IIH one. Let us take a look at how the width of the wave localization region changes along the field line in this case [Mikhailova, 2011].

Return to dispersion relation (5). If we consider it as a biquadratic equation with respect to $k_\parallel$, the solution is written as

$$k_{\parallel 1,2}^2 = \frac{1}{2} \left(2 \frac{\omega^2}{c^2} \varepsilon_\perp - k_\perp^2 \pm \sqrt{k_\perp^4 + 4 \frac{\omega^4}{c^4} \eta^2} \right). \quad (81)$$

Resting on the condition $k_\parallel = 0$, we can find the reflection points bounding the resonator. We have

$$k_\perp^2 = \frac{\omega^2}{c^2} \frac{\varepsilon_\perp^2 - \eta^2}{\varepsilon_\perp}. \quad (82)$$

In the quasi-parallel approximation at $k_\perp = 0$, we obtain the parallel ion-cyclotron resonator whose properties are described in [Guglielmi et al., 2000, 2001; Guglielmi and Kangas, 2007]. In the opposite case, when $k_\perp \to \infty$, we get the resonator for IIH waves [Klimushkin et al., 2010; Mikhailova et al., 2020a, b].

Since we deal with the range that is higher but of the same order of magnitude as the gyrofrequency of heavy ions and much lower than the gyrofrequency of protons ($\Omega_{ch} \le \omega << \Omega_{cp}$), the elements of the permittivity tensor can be written as

$$\varepsilon_\perp = \frac{c^2}{A_p^2} \left[1 + \frac{A_p^2}{A_h^2 \left(1 - \frac{\omega^2}{\Omega_{ch}^2} \right)} \right], \quad (83)$$

$$\eta = \frac{c^2}{\omega} \left[\frac{\Omega_{ce}}{A_e^2} - \frac{\Omega_{cp}}{A_p^2} - \frac{\Omega_{ch}}{A_h^2 \left(1 - \frac{\omega^2}{\Omega_{ch}^2} \right)} \right], \quad (84)$$

Then, function (82) will behave as shown in Figure 10. Function (82) is singular at ω_0. With a wave frequency close to ω_0, the wave is quasi-perpendicular. The frequency ω_0 corresponds to the frequency of the IIH mode

$$\omega_0^2 = \Omega_{ch}^2 \left(1 + \frac{\rho_h}{\rho_p} \right).$$

This expression is the wave frequency at the reflection point for quasi-perpendicular IIH waves (47). The frequencies ω_1 and ω_2 can be found from $\varepsilon_\perp^2 = \eta^2$. These frequencies correspond to the frequencies of quasi-parallel

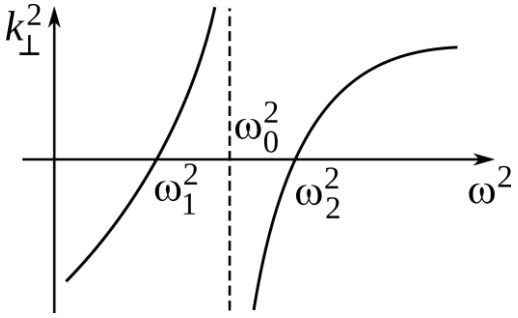

Figure 10. Frequency dependence of the squared perpendicular wave vector component

waves and determine reflection points for the ion-cyclotron resonator.

Accordingly, dimensions of the resonator are also different. The coordinate of the reflection (turning) point changes depending on the wave vector. On different magnetic shells, both the parallel width of the resonator and its dimensions across the magnetic shells change. The half-width of the resonator along the field line is shown in Figure 11. Quasi-parallel ion-cyclotron waves are localized in the region of the resonator bounded by the points l_1 and $-l_1$ (not shown in the Figure), and the region of the equatorial resonator for quasi-perpendicular IIH waves is limited by the points l_0 and $-l_0$ (omitted). Along the field line, the wave can be both quasi-parallel and quasi-perpendicular. The waves differ in frequency, so it would be more correct to speak of the mode conversion from ion-cyclotron to ion-ion hybrid mode. Wave polarization will also change from left-hand circular to linear.

5. DISCUSSION AND CONCLUSION

We have discussed the main theoretical models describing the structure of Pc1 magnetospheric waves. Each subsequent model supplemented and expanded the previous ones. Undoubtedly, a very important step in the study of Pc1 waves was the consideration of the presence of heavy ions in magnetospheric plasma because it turned out that the wave packet in this case is limited in space. The presence of heavy ions leads to localization of both ion cyclotron waves and IIH waves near the equator. Ion-cyclotron waves have left-hand circular polarization, which means that the wave should have both radial E_r and azimuthal E_a components of the electric field. Accordingly, the magnetic field also has both radial and azimuthal components [Guglielmi et al., 2000, 2001; Guglielmi, Potapov, 2012; Mikhailova, 2014]. This distinguishes ion-cyclotron waves from IIH waves. IIH waves are linearly polarized, their electric field oscillates either only in the radial direction (toroidal mode: $E_r >> E_a$, $B_r << B_a$), or only in the azimuthal direction (poloidal mode: $E_r << E_a$, $B_r >> B_a$) [Klimushkin et al., 2010; Mikhailova et al., 2020a].

On the other hand, the poloidal and toroidal IIH-wave modes have properties similar to long-period Alfvén waves, which can also be poloidal and toroidal. However, while in the case of Alfvén waves the entire field line oscillates, in the case of IIH waves only the equatorial part of the field line oscillates (see Figure 6). Like toroidal and poloidal Alfvén waves, IIH modes have different parallel structures and frequencies (polarization splitting of the spectrum). The eigenfrequency of the poloidal IIH mode is lower than that of the toroidal one. The difference between the frequencies is small compared to their values. Due to the similarity between Alfvén waves and IIH modes, we can reasonably expect that the theory developed for Alfvén waves [Leonovich, Mazur, 1993, 1995 , 1997; Klimushkin, 1998; Klimushkin et al., 2004; Mager, Klimushkin, 2013] can be qualitatively applied to IIH waves.

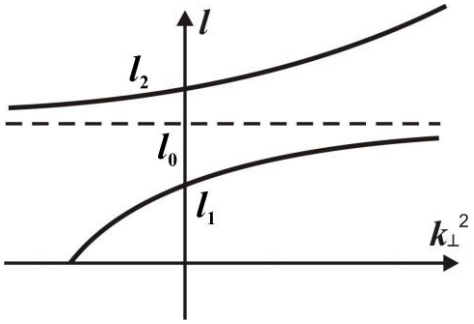

Figure 11. Half-width of the resonator as a function of the squared perpendicular wave vector component [Mikhailova, 2011]

On two different magnetic shells (toroidal x^1_{TN} and poloidal x^1_{PN}), the wave frequency is determined by the expressions

$$\omega = \Omega_{TN}\left(x^1\right), \tag{85}$$

$$\omega = \Omega_{PN}\left(x^1\right). \tag{86}$$

Both coordinates x^1_{TN} and x^1_{PN} depend on the wave frequency ω. Since $\Omega_{PN} < \Omega_{TN}$, the poloidal surface is closer to Earth than the toroidal one: $x^1_{PN}(\omega) < x^1_{TN}(\omega)$.

In the main part of the magnetosphere, the toroidal and poloidal eigenfrequencies of Alfvén waves decrease with distance x^1 from Earth and may have local minima and maxima. Such extrema exist in the regions of the plasmapause, ring current, and also if there are local plasma inhomogeneities (inhomogeneities in proton and heavy ion densities). Then the wave can be trapped in the region of the local minimum of the poloidal eigenfrequency (IIH waves) and in the region of the local maximum of the poloidal eigenfrequency (Alfvén waves). Moreover, the wave can change its polarization from poloidal to toroidal when moving from the poloidal surface to the toroidal one. There are already experimental observations of such a polarization change for Alfvén waves [Leonovich et al., 2015].

The IIH waves have been observed in the magnetosphere of Earth and other planets [Kim et al., 2009, 2015a, b, 2019]. These papers suggest the following mechanism for generating IIH waves: a fast magnetic sound propagates through magnetic shells until it reaches a resonance point due to the presence of ions of two types in the plasma. At the resonance point, due to the mode conversion, the IIH mode is generated. This process is similar to the Alfvén resonance of magnetic field lines. In this case, a toroidal IIH wave is assumed to be generated, but Mikhailova et al. [2020a] have shown that the IIH wave may also be poloidal. In this regard, the question as to how poloidal IIH modes are generated remains open. Their generation is likely to be associated with the resonant interaction of the wave with high-energy charged particles of the ring current, as it occurs for poloidal Alfvén waves. This issue is yet to be explored.

In addition to the reflection points and the IIH resonance points, so-called crossovers also appear. A crossover is a point at which frequencies of left-hand polarized and right-hand polarized ion-cyclotron waves coin-

cide [Rauch, Roux, 1982]. This frequency is determined from Expression (6) at η=0:

$$\omega_{cr}^2 = \frac{n_p}{n_e}\Omega_{ch}^2 + \frac{n_h}{n_e}\Omega_{cp}^2. \quad (87)$$

The question about the role of the crossover in the generation of linearly polarized waves is widely discussed in the literature. For example, Kazakov and Fülöp [2013], having calculated the value $k_\parallel$, at which the mode conversion becomes significant, argue that it always occurs near the crossover frequency ω_{cr}. They suggest that it is possible to estimate the concentration of heavy ions in plasma, using the value of the crossover frequency at the IIH resonance point. However, the IIH resonance can be effective over a wide range of frequencies relative to the crossover frequency. For example, Mercury's magnetosphere features the frequencies $0.5\omega_{cr} \le \omega \le 0.9\omega_{cr}$ [Kim et al., 2011]. Kim and Johnson stated that the crossover frequency cannot be used to determine the concentration of heavy ions in the magnetosphere [Kim, Johnson, 2014]. In more recent works, using computer simulations, Kim et al. agreed that for waves with a wave vector directed along the magnetic field, mode conversion occurs exactly in the crossover region. Nonetheless, with the deviation of the wave vector from parallel (up to normal) when crossing the crossover, no change in the wave polarization occurs [Kim et al., 2015b; Kim and Johnson, 2016]. Therefore, the question about the role of the crossover in mode conversion and hence about its role in the wave energy transfer to Earth's surface is still open.

The resonator features a discrete set of eigenfrequencies. For Pc1 waves there are no observations that clearly demonstrate such a picture, just as there are no observations indicating the existence of the equatorial resonator. There are however observations of long-period Pc4 waves trapped in the resonator and having a quasi-discrete spectrum [Mager et al., 2018]. Pc4 waves are poloidal Alfvén waves, and we have pointed out more than once that their nature is similar to IIH modes. Therefore, the observation of the resonator for Pc4 waves inspires hope that the resonator for IIH waves will be discovered sooner or later.

Finally, Figure 4 shows that in addition to the transparent region there are two more transparent regions at the equator, which are located near the ionosphere of the Southern and Northern hemispheres [Mikhailova, 2011]. These regions are separated from the equatorial resonator by sufficiently wide opaque regions, where $k_\parallel^2 < 0$, and do not have a significant effect on modes in the resonator. Should the opaque regions be narrow, part of the wave energy may leak out of the resonator due to the tunnel effect. In this case, eigenfrequencies in the equatorial resonator will differ from those we calculated and a slight correction will be required.

The work was financially supported by the Ministry of Science and Higher Education of the Russian Federation.

REFERENCES

Abramowitz M., Stegun I.A. *Handbook of mathematical functions with formulas, graphs and mathematical tables*. National Bureau of Standarts Applied Mathematics Series. Washington, 1964.

Anderson B.J., Erlandson R.E., Zanetti L.J. A statistical study of Pc1-2 magnetic pulsations in the equatorial magnetosphere: 1. Equatorial occurrence distributions. *J. Geophys. Res*. 1992a, pp. 3075–3088. DOI: 10.1029/91JA02706.

Anderson B.J., Erlandson R.E., Zanetti L.J. A statistical study of Pc1-2 magnetic pulsations in the equatorial magnetosphere: 2.Wave properties. *J. Geophys. Res*. 1992b, vol. 97, no. A3, pp. 3089–3101. DOI: 10.1029/91JA02697.

Anderson B.J., Denton R.E., Ho G., Hamilton D.C., Fuselier S.A., Strangeway R.J. Observational test of local proton cyclotron instability in the Earth's magnetosphere. *J. Geophys. Res.: Space Phys.* 1996, vol. 101, no. A10, pp. 21527–21543. DOI: 10.1029/96JA01251.

Brunelli B.Ye., Namgaladze A.A. *Fizika ionosfery* [Physics of the Ionosphere]. Moscow, Nauka Publ., 1988, 528 p. (In Russian).

Buchsbaum S.J. Ion resonance in a multicomponent plasma. *Phys. Rev. Lett*. 1960, vol. 5, no. 11, pp. 495–497. DOI: 10.1103/PhysRevLett.5.495.

Chen L., Thorne R.M., Horne R.B. Simulation of EMIC wave excitation in a model magnetosphere including structured high-density plumes. *J. Geophys. Res.: Space Phys*. 2009, vol. 114, no. A7. DOI: 10.1029/2009JA014204.

Cornwall J.M. Cyclotron instabilities and electromagnetic emission in the ultra low frequency and very low frequency ranges. *J. Geophys. Res*. 1965, vol. 70, no. 1, pp. 61–69. DOI: 10.1029/JZ070i001p00061.

Demekhov A.G. Coupling at the atmosphere—ionosphere—magnetosphere interface and resonant phenomena in the ULF Range. *Space Sci. Rev*. 2012, vol. 168, no. 1, pp. 595–609. DOI: 10.1007/s11214-011-9832-6.

Dmitrienko I.S., Mazur V.A. On waveguide propagation of Alfvén waves at the plasmapause. *Planetary Space Sci*. 1985, vol. 33, no. 5, pp. 471–477. DOI: 10.1016/0032-0633(85) 90092-3.

Dmitrienko I.S., Mazur V.A. The spatial structure of quasicircular Alfvén modes of waveguide at the plasmapause — Interpretation of Pc1 pulsations. *Planetary Space Sci*. 1992, vol. 40, pp. 139–148. DOI: 10.1016/0032-0633(92)90156-I.

Engebretson M.J., Peterson W.K., Posch J.L., Klatt M.R., Anderson B.J., Russell C.T., Singer H.J., Arnoldy R.L., Fukunishi H. Observations of two types of Pc1-2 pulsations in the outer dayside magnetosphere. *J. Geophys. Res*. 2002, vol. 107, no. A12. DOI: 10.1029/2001JA000198.

Engebretson M.J., Keiling A., Fornacon K.-H., Cattell C.A., Johnson J.R., Posch J.L., Quick S.R., Glassmeier K.-H., Parks G.K., R'eme H. Cluster observations of Pc1-2 waves and associated ion distributions during the October and November 2003 magnetic storms. *Planetary Space Sci*. 2007, vol. 55, no. 6, pp. 829–848. DOI: 10.1016/j.pss.2006.03.015.

Engebretson M.J., Posch J.L., Westerman A.M., Otto N.J., Slavin J.A., Le G., Strangeway R.J., Lessard M.R. Temporal and spatial characteristics of Pc1 waves observed by ST5. *J. Geophys. Res.: Space Phys*. 2008, vol. 113, no. A7. DOI: 10.1029/2008JA013145.

Farmer W.A., Morales G.J. Propagation of shear Alfvén waves in two-ion species plasmas confined by a nonuniform magnetic field. *Phys. Plasmas*. 2013, vol. 20, no. 8, p. 082132. DOI: 10.1063/1.4819776.

Fedorov E., Mazur N., Pilipenko V., Engebretson M. Interaction of magnetospheric Alfvén waves with the ionosphere in the Pc1 frequency band. *J. Geophys. Res.: Space Phys*. 2016, vol. 121, no. 1, pp. 321–337. DOI: 10.1002/2015JA021020.

Fraser B.J., Nguyen T.S. Is the plasmapause a preferred source region of electromagnetic ion cyclotron waves in the magnetosphere? *J. Atmos. Solar-Terr. Phys*. 2001, vol. 63, pp. 1225–1247. DOI: 10.1016/S1364-6826(00)00225-X.

Fraser B.J., Lotoániu T.M., Singer H.J. Electromagnetic ion cyclotron waves in the magnetosphere. B: Magnetospheric ULF waves: synthesis and new directions. *American Geophysical Union (AGU)*. 2006, pp. 195–212. DOI: 10.1029/169GM13.

Gintzburg M.A. Low-frequency waves in the multicomponent plasma. *Geomagnetizm i aeronomiya* [Geomagnetism and Aeronomy]. 1963, vol. 3, pp.757–761. (In Russian).

Glassmeier K.-H., Mager P.N., Klimushkin D.Yu. Concerning ULF pulsations in Mercury's magnetosphere. *Geophys. Res. Lett.* 2003, vol. 30, no. 18. DOI: 10.1029/2003GL017175.

Glassmeier K.-H., Klimushkin D., Othmer C., Mager. P. ULF waves at Mercury: Earth, the giants, and their little brother compared. *Adv. Space Res*. 2004, vol. 33, pp. 1875–1883. DOI: 10.1016/j.asr.2003.04.047.

Guglielmi A.V. On the nature of hydromagnetic whistlers. *Doklady Akademii Nauk SSSR* []. 1967, vol. 174, no 7, pp. 1076–1078. (In Russian).

Guglielmi A.V. Cyclotron instability of the outer radiation belt protons. *Geomagnetizm i aeronomiya* [Geomagnetism and Aeronomy]. 1968, vol. 8, no. 7, pp. 412–419. (In Russian).

Guglielmi A., Kangas J. Pc1 waves in the system of solar-terrestrial relations: new reflections. *J. Atmos. Solar-Terr. Phys.* 2007, vol. 69, pp. 1635–1643. DOI: 10.1016/j.jastp.2007.01.015.

Guglielmi A.V., Potapov A.S. The effect of heavy ions on the spectrum of oscillations of the magnetosphere. *Kosmicheskie issledovaniya* [Cosmic Res.]. 2012, vol. 50, pp. 283–291. (In Russian).

Guglielmi A.V., Potapov A.S. Problems of the Pc1 magnetospheric wave theory. A review. *Solar-Terr. Phys.* 2019, vol. 5, no. 3, pp. 87–92. DOI: 10.12737/stp-53201910.

Guglielmi A.V., Potapov A.S. Frequency-modulated ULF waves in near-Earth space. *Phys. Usp*. 2021, vol. 64, no. 5, pp. 452–467. DOI: 10.3367/UFNe.2020.06.038777.

Guglielmi A.V., Troitskaya V.A. *Geomagnitnye pulsatsii i diagnostika magnitosfery* [Geomagnetic pulsations and diagnostics of the magnetosphere]. Moscow, Nauka Publ., 1973, 208 p. (In Russian).

Guglielmi A.V., Potapov A.S., Russell C.T. The ion cyclotron resonator in the magnetosphere. *JETP Lett*. 2000, vol. 72, no. 6, p. 298–300.

Guglielmi A., Kangas J., Potapov A. Quasiperiodic modulation of the Pc1 geomagnetic pulsations: an unsettled problem. *J. Geophys. Res*. 2001, vol. 106, no. A11, pp. 25847–25855. DOI: 10.1029/2001JA000136.

Gurnett D.A., Shawhan S.D., Brice N.M., Smith R.L. Ion cyclotron whistlers. *J. Geophys. Res*. 1965, vol. 70, no. 7, pp. 1665–1688. DOI: 10.1029/JZ070i007p01665.

Horne R.B., Thorne R.M. On the preferred source location for the convective amplification of ion cyclotron waves. *J. Geophys. Res.: Space Phys*.1993, vol. 98, no. A6, pp. 9233–9247. DOI: 10.1029/92JA02972.

Horne R.B., Thorne R.M. Wave heating of *He*+ by electromagnetic ion cyclotron waves in the magnetosphere: heating near the *H*+ − *He*+ bi-ion resonance frequency. *J. Geophys. Res.: Space Phys*. 1997, vol. 102, no. A6, pp. 11457–11471. DOI: 10.1029/97JA00749.

Jacobs J.A., Watanabe T. Micropulsation whistlers. *J. Atmos. Terr. Phys*. 1964, vol. 26, no. 8, pp. 825–829. DOI: 10.1016/0021-9169(64)90180-1.

Kazakov Ye.O., Fülöp T. Mode conversion of waves in the ion-cyclotron frequency range in magnetospheric plasmas. *Phys. Rev. Lett.* 2013, vol. 111 (12), p. 125002. DOI: 10.1103/PhysRevLett.111.125002.

Kennel C.F., Petschek H.E. Limit on stably trapped particle fluxes. *J. Geophys. Res*. 1966, vol. 71, no. 1, pp. 1–28. DOI: 10.1029/JZ071i001p00001.

Kim E.-H., Johnson J.R. Comment on mode conversion of waves in the ion-cyclotron frequency range in magnetospheric plasmas. *Phys. Rev. Lett*. 2014, no.113, p. 089501.

Kim E.-H., Johnson J.R. Full-wave modeling of EMIC waves near the *He*+ gyrofrequency. *Geophys. Res. Lett*. 2016, vol. 43, no. 1, pp. 13–21. DOI: 10.1002/2015GL066978.

Kim E.-H., Johnson J.R., Lee D.-H. Resonant absorption of ULF waves at Mercury's magnetosphere. *J. Geophys. Res.: Space Phys*. 2008, vol. 113, no. A11, DOI: 10.1029/2008JA013310.

Kim E.-H., Johnson J.R., Cairns I.H., Lee D.-H. Waves in Space Plasmas. *AIP Conference Proceedings*. 2009, vol. 1187, no. 1, pp. 13–20. DOI: 10.1063/1.3273713.

Kim E.-H., Johnson J.R., Lee D.-H. ULF wave absorption at Mercury. *Geophys. Res. Lett*. 2011, vol. 38, no. 16, p. L16111. DOI: 10.1029/2011GL048621.

Kim E.-H., Johnson J.R., Lee D.-H., Pyo Y.S. Field-line resonance structures in Mercury's multi-ion magnetosphere. Earth, *Planets and Space*. 2013, vol. 65, no. 5, p. 6. DOI: 10.5047/eps.2012.08.004.

Kim E.-H., Johnson J.R., Lee D.-H. Localization of Ultra-Low Frequency Waves in Multi-Ion Plasmas of the Planetary Magnetosphere. *J. Astron. Space Sci*. 2015a, vol. 32, pp. 289–295. DOI: 10.5140/JASS.2015.32.4.289.

Kim E.-H., Johnson J.R., Kim H., Lee D.-H. Inferring magnetospheric heavy ion density using EMIC waves. *J. Geophys. Res.: Space Phys*. 2015b, vol. 120, no. 8, pp. 6464–6473. DOI: 10.1002/2015JA021092.

Kim E.-H., Johnson J.R., Lee D.-H. Electron inertial effects on linearly polarized electromagnetic ion cyclotron waves at Earth's magnetosphere. *J. Geophys. Res.: Space Phys*. 2019, vol. 124, no. 4, pp. 2643–2655. DOI: 10.1029/2019JA026532.

Klimushkin D.Yu. Method of description of the Alfvén and magnetosonic branches of inhomogeneous plasma oscillations. *Plasma Phys. Rep*. 1994, vol. 20, pp. 280–286.

Klimushkin D.Yu. Resonators for hydromagnetic waves in the magnetosphere. *J. Geophys. Res*. 1998, vol. 103, pp. 2369–2375. DOI: 10.1029/97JA02193.

Klimushkin, D.Yu., Mager P.N. The Alfvén mode gyrokinetic equation in finite-pressure magnetospheric plasma. *J. Geophys. Res.: Space Phys*. 2015, vol. 120, pp. 4465–4474. DOI: 10.1002/2015JA021045.

Klimushkin D.Yu., Mager P.N., Glassmeier K.-H. Toroidal and poloidal Alfvén waves with arbitrary azimuthal wave numbers in a finite pressure plasma in the Earth's magnetosphere. *Ann. Geophys*. 2004, vol. 22, ap. 267–288. DOI: 10.5194/angeo-22-267-2004.

Klimushkin D.Yu., Mager P.N., Glassmeier K.-H. Axisymmetric Alfvén resonances in a multi-component plasma at finite ion gyrofrequency. *Ann. Geophys*. 2006, vol. 24, pp. 1077–1084. DOI: 10.5194/angeo-24-1077-2006.

Klimushkin D.Yu., Mager P.N., Marilovtseva O.S. Parallel structure of Pc1 ULF oscillations in multi-ion magnetospheric plasma at finite ion gyrofrequency. *J. Atmos. Solar-Terr. Phys*. 2010, vol. 72, no. 18, pp. 1327–1332. DOI: 10.1016/ j.jastp.2010.09.019.

Krall N., Trivelpiece A.W. *Principles of plasma physics*. McGraw-Hill; First Edition, 1973. 674 p.

Landau L.D., Lifshits E.M. Kurs teoreticheskoi fiziki. Kvantovaya mekhanika (nerelyativistskaya teoriya) [The course of Theoretical Physics. Quantum Mechanics (nonrelativistic theory)]. Fizmalit. 2004, 800 p. (In Russian).

Lee D.-H., Johnson J.R., Kim K., Kim K.-S. Effects of heavy ions on ULF wave resonances near the equatorial region. *J. Geophys. Res.: Space Phys*. 2008, vol. 113, no. A11. DOI: 10.1029/2008JA013088.

Leonovich A.S., Mazur V.A. A theory of transverse small-scale standing Alfvén waves in an axially symmetric magnetosphere. Planetary Space Sci. 1993, vol. 41, pp. 697–717. DOI: 10.1016/0032-0633(93)90055-7.

Leonovich A.S., Mazur V.A. Magnetospheric resonator for transverse-small-scale standing Alfvén waves. *Planetary Space Sci*. 1995, vol. 43, pp. 881–883. DOI: 10.1016/0032-0633(94)00206-7.

Leonovich A.S., Mazur V.A. A model equation for monochromatic standing Alfvén waves in the axially-symmetric magnetosphere. *J. Geophys. Res*. 1997, vol. 102, P. 11443–11456. DOI: 10.1029/96JA02523.

Leonovich A.S., Mazur V.A. *Lineinaya teoriya MGD-kolebanii magnitosfery* [Linear theory of MHD-waves of magnetosphere]. Fizmalit. 2016, 480 p. (In Russian).

Leonovich A.S., Klimushkin D.Yu., Mager P.N. Experimental evidence for the existence of monochromatic transverse small-scale standing Alfvén waves with spatially dependent polarization. *J. Geophys. Res.: Space Phys*. 2015, vol. 120. P. 5443–5454. DOI: 10.1002/2015JA021044.

Lessard M.R., Lund E.J., Kim H.M. Pi1B pulsations as a possible driver of Alfvénic aurora at substorm onset. *J. Geophys. Res.: Space Phys.* 2011, vol. 116, no. A6. DOI: 10.1029/2010JA015776.

Lotoaniu T.M. Propagation of electromagnetic ion cyclotron wave energy in the magnetosphere. *J. Geophys. Res.: Space Phys.* 2005, vol. 110, iss. A7. CiteID A07214. DOI: 10.1029/ 2004JA010816.

Lundin R., Guglielmi A. Ponderomotive forces in cosmos. *Space Sci. Rev*. 2006, vol. 127, pp. 1–116. DOI: 10.1007/s11214-006-8314-8.

Mager P.N., Klimushkin D.Yu. Giant pulsations as modes of a transverse Alfvénic resonator on the plasmapause. *Earth, Planets and Space*. 2013, vol. 65, pp. 397–409. DOI: 10.5047/eps. 2012.10.002.

Mager P.N., Mikhailova O.S., Mager O.V., Klimushkin D.Yu. Eigenmodes of the transverse Alfvénic resonator at the plasmapause: a Van Allen Probes case study. *Geophys. Res. Lett*. 2018, vol. 45, pp. 10,796—10,804. DOI: 10.1029/2018GL079596.

Mikhailova O.S. On the possibility of localisation of Pc1 waves nearby the ionosphere, taking account of heavy ions in the magnetosphere. *Solnechno-zemnaya fizika* [Solar-Terrestrial Phys.]. 2011, vol. 19, pp. 83–87. (In Russian).

Mikhailova O.S. Studing the structure of ULF oscillations near the plasmapause, given heavy ions in magnetospheric plasma. *Solnechno-zemnaya fizika* [Solar-Terrestrial Phys.]. 2013, vol. 23, pp. 84–90. (In Russian).

Mikhailova O.S. The spatial structure of ULF-waves in the equatorial resonator localized at the plasmapause with the admixture of the heavy ions. *J. Atmos. Solar-Terr. Phys*. 2014, vol. 108, pp. 10–16. DOI: 10.1016/j.jastp.2013.12.007.

Mikhailova O.S., Mager P.N., Klimushkin D.Yu. Two modes of ion-ion hybrid waves in magnetospheric plasma. *Plasma Physics and Controlled Fusion*. 2020a, vol. 62, no. 2, p. 025026. DOI: 10.1088/1361-6587/ab5b32.

Mikhailova O.S., Mager P.N., Klimushkin D. Yu. Transverse resonator for ion-ion hybrid waves in dipole magnetospheric plasma. *Plasma Physics and Controlled Fusion*. 2020b, vol. 62, no. 9, p. 095008. DOI: 10.1088/1361-6587/ab9be9.

Mishin V.V., Lunyushkin S.B., Mikhalev A.V., Klibanova Yu.Yu., Tsegmed B., Karavaev Yu.A., Tashchilin A.V., Leonovich L.A., Penskikh Yu.V. Extreme geomagnetic and optical disturbances over Irkutsk during the 2003 November 20 superstorm. *J. Atmos. Solar-Terr. Phys*. 2018, vol. 181, pp. 68–78. DOI: 10.1016/j.jastp.2018.10.013.

Mishin V.V., Tsegmed B., Klibanova Yu.Yu., Kurikalova M.A. Burst geomagnetic pulsations as indicators of substorm expansion onsets during storms. *J. Geophys. Res.: Space Phys*. 2020, vol. 125, no. 10. DOI: 10.1029/2020JA028521.

Mithaiwala M., Rudakov L., Ganguli G. Generation of a ULF wave resonator in the magnetosphere by neutral gas release. *J. Geophys. Res.: Space Phys*. 2007, vol. 112, no. A9, p. A09218. DOI: 10.1029/2007JA012445.

Mursula K. Satellite observations of Pc1 pearl waves: The changing paradigm. *J. Atmos. Solar-Terr. Phys*. 2007, vol. 69, no. 14, pp. 1623–1634. DOI: 10.1016/j.jastp.2007.02.013.

Mursula K., Blomberg L.G., Lindqvist P.-A., Marklund G.T., Bräysy T., Rasinkangas R., Tanskanen P. Dispersive Pc1 bursts observed by Freja. *Geophys. Res. Lett*. 1994, vol. 21, no.17, pp. 1851–1854. DOI: 10.1029/94GL01584.

Mursula K., Bräysy T., Niskala K., Marklund G.T., Bräysy T., Rasinkangas R., Tanskanen P. Pc1 pearls revisited: Structured electromagnetic ion cyclotron waves on Polar satellite and on ground. *J. Geophys. Res.: Space Phys*. 2001, vol. 106, no. A12, pp. 29543–29553. DOI: 10.1029/2000JA003044.

Obayashi T. Hydromagnetic whistlers. *J. Geophys. Res.* 1965, vol. 70, no. 5, pp. 1069–1078. DOI: 10.1029/JZ070i005p01069.

Polyakov A.R. The structure of equidistant-frequency groups in the oscillation spectra of the dayside magnetosphere. *J. Atmos. Solar-Terr. Phys*. 2019, vol. 189, pp. 44–51. DOI: 10.1016/j.jastp.2019.04.008.

Rauch J.L., Roux A. Ray tracing of ULF waves in a multicomponent magnetospheric plasma: Consequences for the generation mechanism of ion cyclotron waves. *J. Geophys. Res*. 1982, vol. 87, no. A10, pp. 8191–8198. DOI: 10.1029/JA087iA10p08191.

Smith R.L., Brice N. Propagation in multicomponent plasmas. *J. Geophys. Res*. 1964, vol. 69, no. 23, pp. 5029–5040. DOI: 10.1029/JZ069i023p05029.

Southwood D.J., Saunders M.A. Curvature coupling of slow and Alfvén MHD waves in a magnetotail field configuration. *Planetary Space Sci*. 1985, vol. 33, pp. 127–134. DOI: 10.1016/0032-0633(85)90149-7.

Sucksdorff E. Occurrences of rapid micropulsations at Sodankylä during 1932 to 1935. *Terrestrial Magnetism and Atmospheric Electricity*. 1936, vol. 41, no. 4, pp. 337–344. DOI: 10.1029/TE041i004p00337.

Swanson D.G. *Plasma Waves*. 2nd Edition. *Bristol: IOP*, 2003. DOI: 10.1201/b15744.

Takahashi K., Denton R.E., Anderson R.R., Hughes W.J. Mass density inferred from toroidal wave frequencies and its comparison to electron density. *J. Geophys. Res.: Space Phys.* 2006, vol. 111, iss. A1. CiteID A01201. DOI: 10.1029/2005JA011286.

Tamao T. Magnetosphere—ionosphere interaction through hydromagnetic waves. *Achievements of the International Magnetospheric Study (IMS)*. 1984, pp. 427–435. (ESA Special Publication, vol. 217).

Usanova M.E., Drozdov A., Orlova K., et al. Effect of EMIC waves on relativistic and ultrarelativistic electron populations: Ground-based and Van Allen Probes observations. *Geophys. Res. Lett*. 2014, vol. 41, no. 5, pp. 1375–1381. DOI: 10.1002/2013GL059024.

Yahnin A.G., Yahnina T.A., Frey H.U. Subauroral proton spots visualize the Pc1 source. *J. Geophys. Res.: Space Phys*. 2007, vol. 112, no. A10. DOI: 10.1029/2007JA012501.

Yang B., Zong Q.-G., Wang Y.F., Fu Y., Song P., Fu H.S., Korth A., Tian T., Reme H. Cluster observations of simultaneous resonant interactions of ULF waves with energetic electrons and thermal ion species in the inner magnetosphere. *J. Geophys. Res.: Space Phys.* 2010, vol. 115, no. A2, DOI: 10.1029/2009JA014542.

Yeoman T.K., James M., Mager P.N., Klimushkin D.Yu. SuperDARN observations of high-*m* ULF waves with curved phase fronts and their interpretation in terms of transverse

resonator theory. *J. Geophys. Res*. 2012, vol. 117, p. A06231. DOI: 10.1029/ 2012JA017668.

Young D.T., Perraut S., Roux A., Villedary C., Gendrin R., Korth A., Kremser G., Jones D. Wave-particle interactions near ω*He*+ observed on GEOS 1 and 2: 1. Propagation of ion cyclotron waves in *He*+-rich plasma. *J. Geophys. Res.: Space Phys*. 1981, vol. 86, no. A8, pp. 6755–6772. DOI: 10.1029/JA086iA08p06755.

Original Russian version: O.S. Mikhailova, D.Yu. Klimushkin, P.N. Mager, published in Solnechno-zemnaya fizika. 2022. Vol. 8. Iss. 1. P. 3–18. DOI: 10.12737/szf-81202201.

How to cite this article

Mikhailova O.S., Klimushkin D.Yu., Mager P.N. The current state of the theory of Pc1 range ULF pulsations in magnetospheric plasma with heavy ions: A review. *Solar-Terrestrial Physics.* 2022. Vol. 8. Iss. 1. P. 3–18. DOI: 10.12737/stp-81202201.